Available online at www.sciencedirect.com

SCIENCE DIRECT®

International Journal of Rock Mechanics & Mining Sciences 41 (2004) 1087–1107

International Journal of Rock Mechanics and Mining Sciences

www.elsevier.com/locate/ijrmms

Modeling non-linear displacement time series of geo-materials using evolutionary support vector machines

Xia-Ting Feng*, Hongbo Zhao, Shaojun Li

Institute of Rock and Soil Mechanics, The Chinese Academy of Sciences, Wuhan 430071, People's Republic of China

Accepted 19 April 2004

Available online 17 June 2004

Abstract

Evaluation of the non-linear deformation behavior of geo-materials is an important aspect of the safety assessment for geotechnical engineering in complex conditions. This paper presents a novel machine learning method, termed support vector machine (SVM), to obtain a global optimization model in conditions of large project dimensions, small sample sizes and non-linearity. A new idea is put forward to combine the SVM with a genetic algorithm. The method has been used in the analysis of the high rock slope of the permanent shiplock of the Three Gorges Project and the horizontal deformation at depth in the Bachimen landslide in Fujian Province, China. The 92 non-linear SVMs in total were constructed with their kernel functions and the parameters were recognized using a genetic algorithm. The results indicate that the established SVMs can appropriately describe the evolutionary law of deformation of geo-materials at depth and provide predictions for the future 6–10 time steps with acceptable accuracy and confidence.

Keywords: Evolutionary support vector machine; Genetic algorithm; Slope; Tunnel; Non-linear time series; Displacement

1. Introduction

Evaluation of the non-linear deformation behavior of geo-materials is an important aspect of the safety assessment for geotechnical engineering in complex conditions. In line with the implementation of the general development strategy in Western China, there are many large-scale rock engineering projects being built and to be built in complex conditions, such as the Three Gorges Project, the Qinghai–Tibet Rail Road, the South–North water transfer project and the West–East gas transfer project. The deformation behavior of large-scale rock masses is aggravated by complex rock structures, excavation blasting, reinforcements, seismic forces, tectonic activities, high stresses, high water pressure, temperature gradient, strong geo-chemical reaction and their coupled effects. The deformation behavior of rock under such complicated circumstances is complex, evolutionary, and is a non-linear dynamic system. The displacement, stresses and acoustic emission in such systems are inherently noisy, non-stationary, and deterministically chaotic. This means that the distribution of displacements is variable over time. Not only is a single data series non-stationary in terms of its mean and variance, but also its relation with other related data series is variable over time. Modeling such dynamic and non-stationary time series is a challenging task. The structure of the model and its parameters cannot be easily determined from prior knowledge in a straightforward fashion.

Over the past few years, neural networks have been successfully used for modeling non-linear time series of rock behavior, such as roof pressure [1], acoustic emission [2–5], and displacement [6]. Neural networks are universal functional approximators capable of mapping any non-linear function without prior assumptions relating to the data [4]. Unlike traditional statistical models, neural networks are data-driven models. Therefore, neural networks are less susceptible

*Corresponding author. Tel.: +86-27-871-989-13; fax: +86-27-871-973-86.

E-mail address: xtfeng@whrsm.ac.cn (X.-T. Feng).

1365-1609/$ - see front matter
doi:10.1016/j.ijrmms.2004.04.003

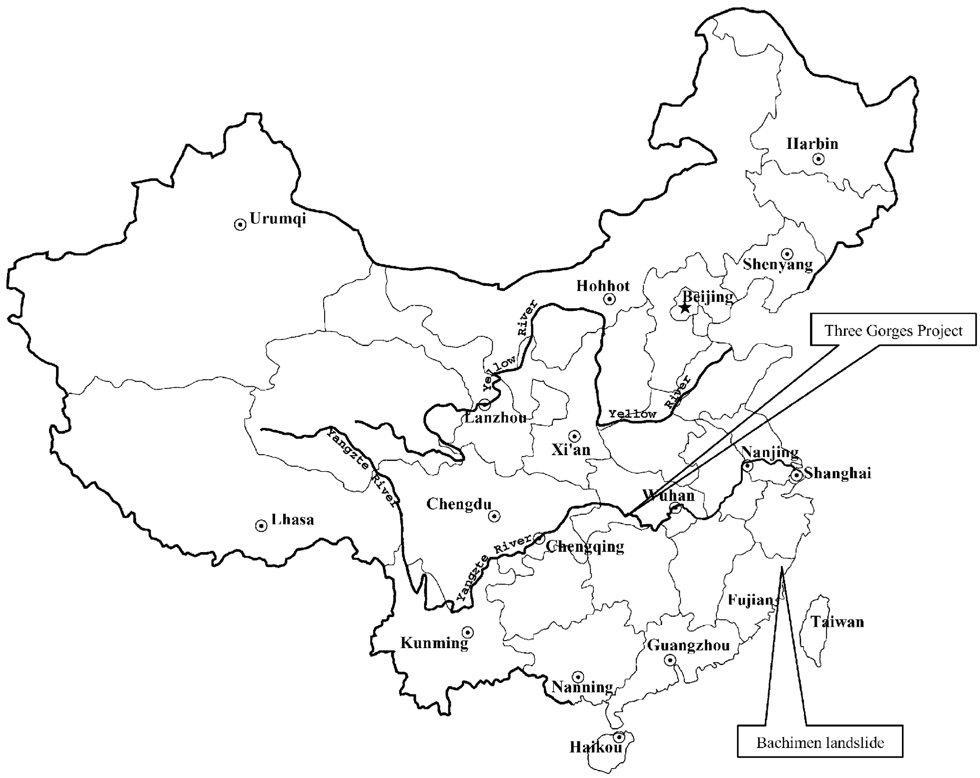

Fig. 1. Locations of case studies for modeling of SVMs for non-linear displacement time series.

to model conceptualization errors than the traditional parametric models, and they are more powerful in describing the dynamics of, for example, displacement/stress/acoustic emission time series than traditional statistical models [1–7].

A novel machine learning method, termed support vector machines (SVMs), was proposed by Vapnik and his co-workers in 1995 [8,9]. This is a new generation learning system based on advances in statistical learning theory, enabling non-linear mapping of an n-dimensional input space into a higher-dimensional feature space where, for example, a linear classifier can be used. The SVM can train non-linear models based on the structural risk minimization principle that seeks to minimize an upper bound of the generalization error rather than minimize the empirical error as implemented in other neural networks. This induction principle is based on the fact that the generalization error is bounded by the sum of the empirical error and a confidence interval term depending on the Vapnik–Chervonenkis (VC) dimension. Based on this principle, SVMs will achieve an optimal model structure by establishing a proper balance between the empirical error and the VC-confidence interval, leading eventually to a better generalization performance than other neural network models. An additional merit of SVMs is that training SVMs is a uniquely solvable quadratic optimization problem, and the complexity of the solution in SVMs depends only on the complexity of the desired solution, rather than on the dimensionality of the input space. Thus, SVMs use a non-linear mapping, based on a kernel function, to transform an input space to a high-dimension space and then look for a non-linear relation between inputs and outputs in the higher dimension space. SVMs not only have a rigorous theoretical background but also can find global optimal solutions for problems with small training samples, high dimension, non-linearity and local optima. Originally, SVMs were developed for pattern recognition problems [10–12]. Recently, SVMs have been shown to give good performance for a wide variety of problems, such as non-linear regression [12–15,9]. A genetic algorithm is a global optimization algorithm [16]. Genetic algorithms can be used to automatically recognize kernel functions and parameters of support vector machines.

In this paper, the evolutionary SVMs are modified to model non-linear displacement of rocks under complex conditions. The models have been tested by modeling non-linear displacement time series of the high slope of the permanent shiplock of the Three Gorges Project and a large landslide in China. The predicted displacement time series are compared with those of the measured ones, with good agreement.

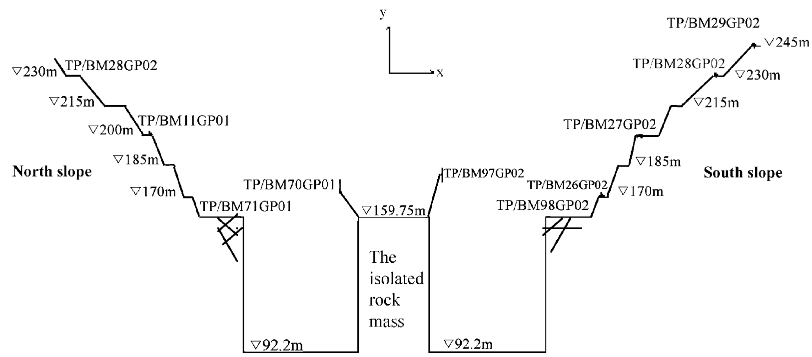

Fig. 2. Locations of displacement monitoring points at Section 17-17 of permanent shiplock slope, Three Gorges Project, China.

Table 1
Parameters of SVMs for each monitoring point at Section 17-17 of permanent shiplock slope, Three Gorges Project, China

Stage	Parameters of SVM	Monitoring point			
		TP/BM11GP01	TP/BM26GP02	TP/BM27GP02	TP/BM29GP02
1	σ	275	211	101	67
	C	3091	4846	3376	2813
	b	0.60	2.08	1.25	10.34
2	σ	151	53	209	49
	C	3181	2259	2642	4132
	b	6.72	5.52	4.18	8.32
3	σ				89
	C				3627
	b				9.94

2. Theory of SVMs

2.1. SVMs for regression

With regard to using the support vector machines for regression, first use a linear function $f(x) = w \cdot x + b$ to regress the data set $\{x_i, y_i\}, i = 1, 2, \ldots, n,\ x_i \in R^n, y_i \in R$. Error-free fitting by the linear function with accuracy ε is assumed to train all the data through

$$\begin{aligned} &y_i - w \cdot x_i - b \leqslant \varepsilon, \quad i = 1, ..., n. \\ &w \cdot x_i + b - y_i \leqslant \varepsilon, \end{aligned} \tag{1}$$

In view of the tolerable error by introducing two relaxation factors, $\xi_i \geqslant 0$ and $\xi_i^* \geqslant 0$, Eq. (1) becomes:

$$\begin{aligned} &y_i - w \cdot x_i - b \leqslant \varepsilon + \xi_i, \quad i = 1, ..., n. \\ &w \cdot x_i + b - y_i \leqslant \varepsilon + \xi_i^*, \end{aligned} \tag{2}$$

The optimum objective is the minimization of $\frac{1}{2}\|w\|^2 + C\sum_{i=1}^{n}(\xi_i + \xi_i^*)$, where the constant $C > 0$ stands for the penalty degree of the sample with error exceeding ε.

A dual problem can then be derived by using the optimization method to maximize the function

$$\begin{aligned} W(\alpha, \alpha^*) = &-\frac{1}{2}\sum_{i,j=1}^{n}(\alpha_i - \alpha_i^*)(\alpha_j - \alpha_j^*)(x_i \cdot x_j) \\ &+ \sum_{i=1}^{n} y_i(\alpha_i - \alpha_i^*) - \varepsilon \sum_{i=1}^{n}(\alpha_i + \alpha_i^*) \end{aligned} \tag{3}$$

subject to the conditions

$$\begin{aligned} &\sum_{i=1}^{n}(\alpha_i - \alpha_i^*) = 0, \\ &0 \leqslant \alpha_i, \alpha_i^* \leqslant C, i = 1, 2, ..., n, \end{aligned} \tag{4}$$

where α_i, α_i^* are Lagrange multipliers.

The SVMs for function fitting obtained by using the above-mentioned maximization function is then given by

$$f(x) = (w \cdot x) + b = \sum_{i=1}^{k}(\alpha_i - \alpha_i^*)(x \cdot x_i) + b, \tag{5}$$

Table 2
Values of Lagrange multipliers of SVMs for each monitoring point at Section 17-17 of permanent shiplock slope, Three Gorges Project, China

Stage	Sample no	Monitoring point no.							
		TPBM11GP01		TPBM26GP02		TPBM27GP02		TPBM29GP02	
		α	α^*	α	α^*	α	α^*	α	α^*
1	1	0.00	3091.00	0.00	4846.00	0.00	3376.00	0.00	1280.39
	2	0.00	3091.00	0.00	4846.00	1043.24	0.00	700.38	0.00
	3	3091.00	0.00	4846.00	0.00	0.00	3376.00	0.00	2813.00
	4	0.00	0.00	0.00	0.00	0.00	3376.00	2813.00	0.00
	5	0.00	0.00	0.00	0.00	3376.00	0.00	1239.45	0.00
	6	0.00	0.00	0.00	0.00	3376.00	0.00	2258.57	0.00
	7	0.00	0.00	0.00	0.00	0.00	3376.00	3.67	0.00
	8	0.00	0.00	4846.00	0.00	1664.64	0.00	133.52	0.00
	9	0.00	0.00	0.00	0.00	3376.00	0.00	0.00	2813.00
	10	0.00	0.00	0.00	0.00	3376.00	0.00	624.36	0.00
	11	1014.29	0.00			0.00	668.10	0.00	1725.77
	12	698.59	0.00			3376.00	0.00	0.00	1764.77
	13	0.00	1712.88			0.00	3376.00	0.00	2813.00
	14	0.00	0.00			0.00	3376.00	0.00	374.83
	15	0.00	0.00			0.00	3376.00	578.16	0.00
	16	0.00	0.00			3376.00	0.00	0.00	878.85
	17	0.00	0.00			0.00	3376.00	2230.75	0.00
	18	0.00	0.00			3376.00	0.00	2813.00	0.00
	19	3091.00	0.00			0.00	2039.77	0.00	1744.24
	20	0.00	0.00			3376.00	0.00	2813.00	0.00
2	1	0.00	3181.00	0.00	904.28	0.00	1158.59	231.26	0.00
	2	3181.00	0.00	2256.37	0.00	2642.00	0.00	0.00	0.00
	3	0.00	438.78	0.00	2259.00	0.00	2642.00	0.00	4132.00
	4	0.00	2144.25	1170.77	0.00	0.00	2642.00	0.00	4132.00
	5	0.00	0.00	0.00	1647.70	0.00	2642.00	1863.82	0.00
	6	0.00	0.00	446.42	0.00	0.00	2642.00	0.00	1280.00
	7	0.00	0.00	913.23	0.00	0.00	2642.00	4132.00	0.00
	8	2144.25	0.00	591.50	0.00	2642.00	0.00	4132.00	0.00
	9	0.00	0.00	19.33	0.00	2624.06	0.00	0.00	3105.38
	10	0.00	0.00	0.00	586.65	2642.00	0.00	3209.33	0.00
	11	608.43	0.00			2642.00	0.00	0.00	495.97
	12	194.12	0.00			0.00	2642.00	4132.00	0.00
	13	0.00	413.32			2642.00	0.00	0.00	1376.49
	14	458.34	0.00			2642.00	0.00	0.00	2277.77
	15	355.15	0.00			0.00	2642.00	0.00	4132.00
	16	630.69	0.00			2642.00	0.00	644.80	0.00
	17	0.00	1019.38			0.00	2642.00	0.00	3610.98
	18	300.43	0.00			2642.00	00.00	2070.20	0.00
	19	0.00	675.68			1076.50	0.00	4132.00	0.00
	20	0.00	0.00			0.00	2541.97	0.00	4.09
3	1							0.00	1726.72
	2							3627.00	0.00
	3							0.00	3627.00
	4							0.00	3627.00
	5							0.00	2239.91
	6							66.54	0.00
	7							0.00	3627.00
	8							563.26	0.00
	9							2668.82	0.00
	10							1090.00	0.00
	11							3627.00	0.00
	12							2337.51	0.00
	13							1896.87	0.00
	14							3627.00	0.00
	15							0.00	900.24
	16							0.00	3197.02
	17							0.00	1311.47
	18							0.00	695.44
	19							495.23	0.00
	20							952.56	0.00

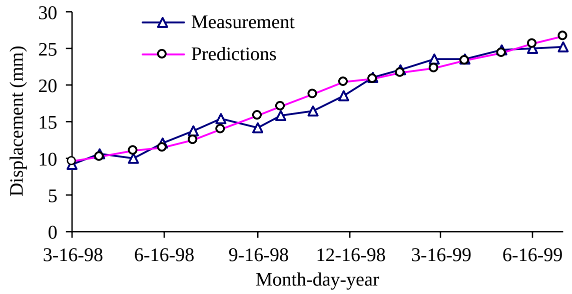

Fig. 3. Comparison of measured and predicted displacements at monitoring point TP/BM11GP01, Section 17-17 of permanent ship-lock slope, Three Gorges Project, China. Stage 1: predictions during 3-16-1998 to 11-9-1998 using the model obtained by learning measured displacements from 1-15-1996 to 2-14-1998. Stage 2: predictions during 12-10-1998 to 7-15-1999 using the model obtained by learning measured displacement from 10-15-1996 to 11-9-1998.

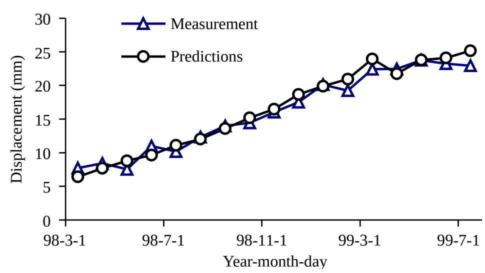

Fig. 4. Comparison of measured and predicted displacements at monitoring point TP/BM26GP02, Section 17-17 of permanent ship-lock slope, Three Gorges Project, China. Stage 1: predictions during 3-16-1998 to 11-9-1998 using the model obtained by learning measured displacements from 11-15-1996 to 2-14-1998 and Stage 2: predictions during 12-10-1998 to 7-15-1999 using the model obtained by learning measured displacements from 8-16-1997 to 11-9-1998.

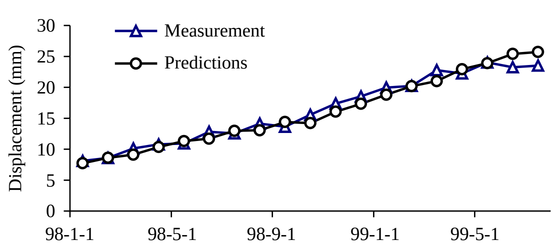

Fig. 5. Comparison of measured and predicted displacements at monitoring point TP/BM27GP02, Section 17-17 of permanent ship-lock slope, Three Gorges Project, China. Stage 1: predictions during 1-14-1998 to 10-8-1998 using the model obtained by learning measured displacements from 11-15-1995 to 12-10-1997 and Stage 2: predictions during 11-9-1998 to 7-15-1999 using the model obtained by learning measured displacements from 9-15-1996 to 10-8-1998.

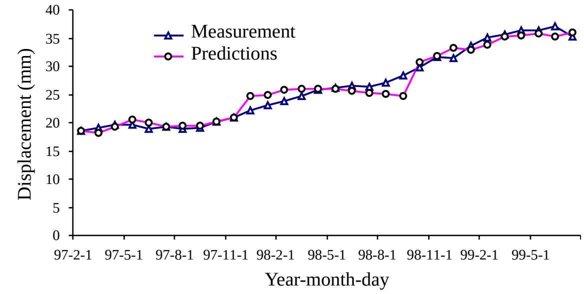

Fig. 6. Comparison of measured and predicted displacements at monitoring point TP/BM29GP02, Section 17-17 of permanent ship-lock slope, Three Gorges Project, China. Stage 1: predictions during 2-1-1997 to 11-1-1997 using the model obtained by learning measured displacements from 12-15-1994 to 1-14-1997, Stage 2: predictions during 12-1-1997 to 9-1-1998 using the model obtained by learning measured displacements from 10-15-1995 to 11-1-1997, and Stage 3: predictions during 10-1-1998 to 7-1-1999 using the model obtained by learning measured displacements from 2-15-1997 to 9-1-1998.

where k is the number of support vectors, b is a constant to be determined during the optimization. Only part of α_i, α_i^* has non-zero values. The sample corresponding to α_i, α_i^* is the support vector to be sought.

As for the non-linear problems, the solution can be found by mapping the original problem to the linear problem in a characteristic space of high dimension, where dot product manipulation can be substituted by a kernel function, i.e. $K(x_i, x_j) = \phi(x_i)\phi(x_j)$. The kernel function can be represented by functions in the original space. Therefore, we are not obliged to know the concrete form of the non-linear mapping and Eqs. (3)–(5) may take the following expressions:

$$W(\alpha, \alpha^*) = -\frac{1}{2}\sum_{i,j=1}^{n}(\alpha_i - \alpha_i^*)(\alpha_j - \alpha_j^*)K(x_i \cdot x_j) + \sum_{i=1}^{n} y_i(\alpha_i - \alpha_i^*) - \varepsilon \sum_{i=1}^{n} (\alpha_i + \alpha_i^*), \quad (6)$$

$$\sum_{i=1}^{n}\left(\alpha_i - \alpha_i^*\right) = 0,$$
$$0 \leqslant \alpha_i, \alpha_i^* \leqslant C, i = 1, 2, \ldots, n, \quad (7)$$

$$f(x) = (w \cdot x) + b = \sum_{i=1}^{k}(\alpha_i - \alpha_i^*)K(x \cdot x_i) + b, \quad (8)$$

where $K(x \cdot x_i)$ is a kernel function which measures the similarity or distance between the input vector x_i and the stored training vector x. Common examples of $K(\cdot)$ are the polynomial kernel function $K(x, y) = ((x \cdot y) + 1)^d, d = 1, 2, \ldots, n$, Gaussian radial base kernel function $K(x, y) = \exp\{-|x - y|^2/\sigma^2\}$, and Sigmoid kernel function $K(x, y) = \tanh(\phi(x \cdot y) + \theta)$, where d, σ are constants.

The common algorithms for solving the quadratic programming problem expressed by Eqs. (3) and (4), (6)

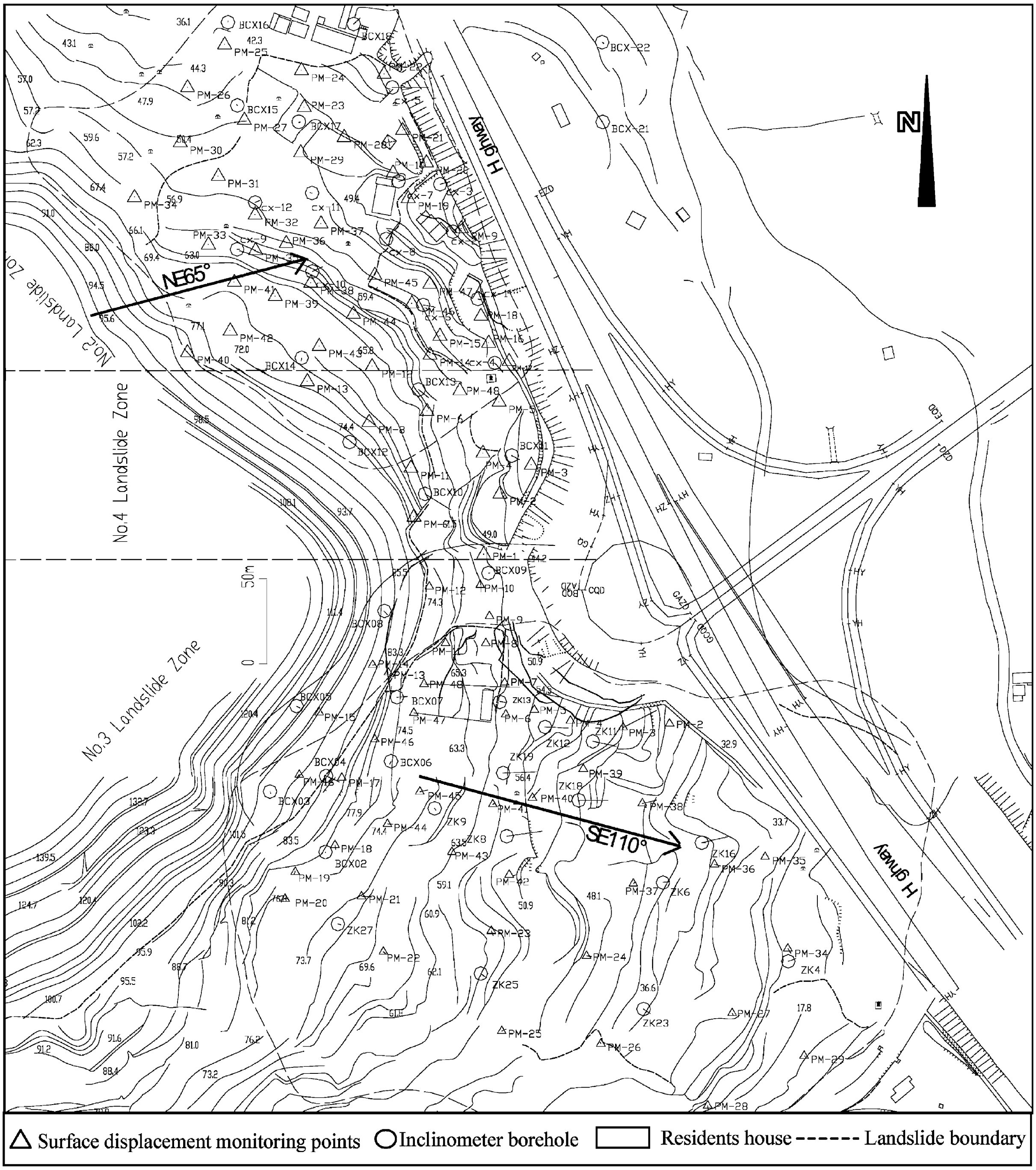

Fig. 7. Location of monitoring points for geo-surface and monitoring boreholes for displacement at No.2 Bachimen landslide, Funing expressway, Fujian, China.

and (7), are the interior point algorithm, sequential minimal optimization algorithm, and decompose algorithm.

2.2. Sequential minimal optimization

Platt has proposed a new algorithm for training SVMs, called Sequential Minimal Optimization (SMO)[17]. It is a simple algorithm that can quickly solve the SVM quadratic programming problem without any extra matrix storage and is exempt from using any numerical quadratic programming optimization steps. SMO decomposes the overall quadratic programming problem into sub-problems of quadratic programming by using Osuna's theorem to ensure convergence. There are two components in SMO: an

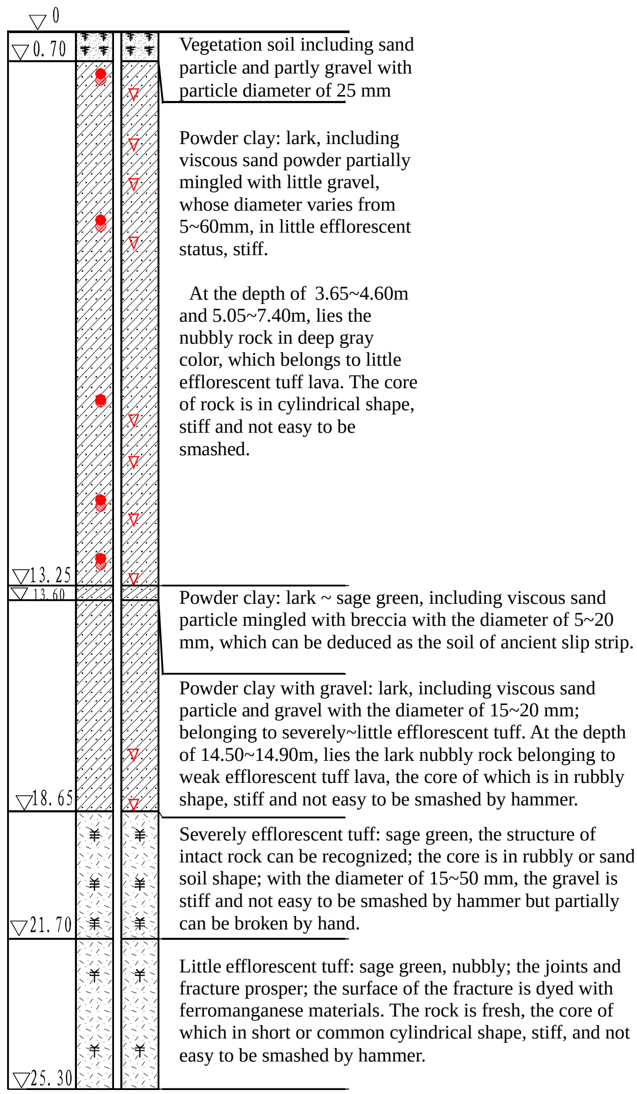

Fig. 8. Geological section of inclinometer borehole cx9 at No.2 Bachimen landslide, Funing expressway, Fujian, China.

analytic method for solving for the two Lagrange multipliers; and a heuristic one for choosing multipliers in optimization.

The advantage of SMO lies in the fact that solving for two Lagrange multipliers can be done analytically. Thus, numerical quadratic programming optimization is avoided completely. The inner loop of the algorithm can be expressed in a small *C* code, rather than invoking an entire quadratic programming library routine. Even though more optimization sub-problems are needed in the solving algorithm, the overall CPU time expense is much reduced due to the quick solution of each sub-problem. In addition, SMO requires no extra matrix storage. Thus, very large SVM training problems can fit inside the memory of an ordinary personal computer or workstation. Because no matrix algorithm is involved in SMO, it is less susceptible to numerical precision problems [17].

The algorithm can be summarized as follows:

(1) Construct the corresponding quadratic optimization model based on the SVM principle.
(2) Assign initial values to the Lagrange multipliers α_i, α_i^* and form the Lagrange multipliers set. Calculate the b value.
(3) Verify whether all the Lagrange multipliers satisfy the Karush–Kuhn–Tucker (KKT) conditions. If all of them are satisfied, then the current values of Lagrange multipliers and b are the solution of the quadratic optimum problem. Otherwise go to step 4).
(4) Select another pair of Lagrange multipliers α_i, α_i^* and verify if it satisfies the KKT conditions. If they are satisfied, then they are selected as the final Lagrange multipliers α_i, α_i^*. Otherwise the current selected pair of Lagrange multipliers α_i, α_i^* is the first multipliers pair.
(5) Use the same procedure to select the second multipliers pair.
(6) Solve the quadratic optimum problem using the above-derived two multipliers pairs. Obtain the new values of the two pairs of Lagrange multipliers and compute b.
(7) Substitute the original values of the two pairs of Lagrange multipliers with their new values and form a new Lagrange multipliers set, then go to step 3).

3. Application of SVMs for non-linear displacement time series

3.1. SVM representation of non-linear displacement time series

A non-linear displacement time-dependent series $\{x_t\} = (x_1, x_2, \ldots, x_n)$ can be obtained by monitoring in geo-materials. Modeling the non-linear displacement series means finding the relation between the displacement x_{i+p} at time $i+p$ and its displacements $x_i, x_{i+1}, \ldots, x_{i+p-1}$ at the previous p time steps, i.e. $x_{i+p} = f(x_i, x_{i+1}, \ldots, x_{i+p-1})$. As a non-linear function, $f(\cdot)$ expresses the non-linear relations of the displacement time series.

According to the theory of SVMs, the above-mentioned non-linear relation can be obtained by learning the measured displacements using the SVMs. That is to say the non-linear relation of the displacement time series can be obtained by learning the displacement behaviour at *n*–*p* time steps

$X_i, X_{i+1}, \ldots, X_{i+p-1} (i = 1, \ldots, n-p)$, i.e.:

$$\hat{X}_{n+m} = \sum_{i=1}^{n-p} (\alpha_i - \alpha_i^*) K(X_{n+m}, X_i) + b \quad m = 1, \ldots, w, \tag{9}$$

where, $\hat{X}_{n+m}$ is the displacement at time $n+m$ X_{n+m} is a displacement series $X_{n+m} = (x_{n+m-p}, x_{n+m-p+1}, \ldots, x_{n+m-1})$, m=1,2,…,wX_i is the displacement !series used as the training samples, $X_i = (x_i, x_{i+1}, \ldots, x_{i+p-1})(i = 1, 2, \ldots, n-p)$. $K(\cdot)$ is the kernel function and w is the number of the future time steps. p is the number of historical points. α, α^* and b are obtained by solving the following quadratic programming problem:

$$W(\alpha, \alpha^*) = -\frac{1}{2} \sum_{i,j=1}^{n-p} (\alpha_i - \alpha_i^*)(\alpha_j - \alpha_j^*) K(X_i \cdot X_j) + \sum_{i=1}^{n-p} X_i(\alpha_i - \alpha_i^*) - \varepsilon \sum_{i=1}^{n-p} (\alpha_i + \alpha_i^*)$$

$$\text{Subject to} \quad \sum_{i=1}^{n-p} (\alpha_i - \alpha_i^*) = 0, \quad 0 \leqslant \alpha_i, \alpha_i^* \leqslant C, i = 1, 2, \ldots, n-p. \tag{10}$$

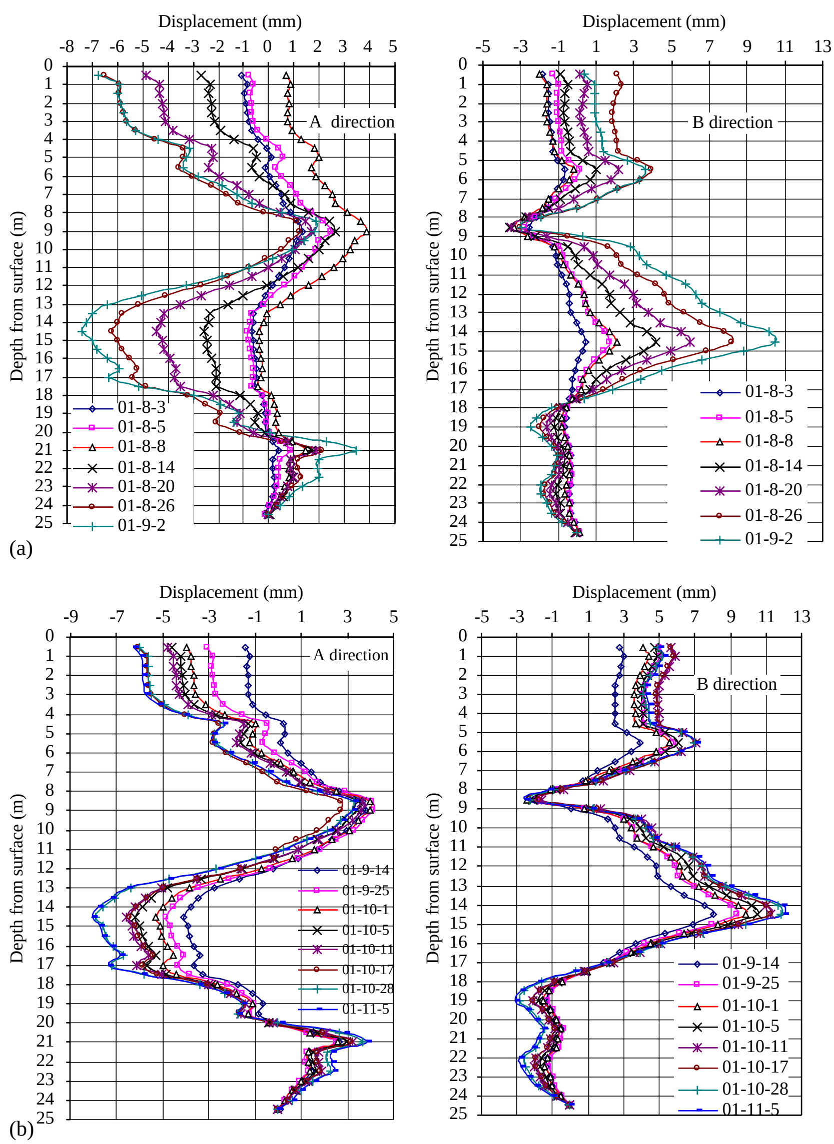

Fig. 9. Monitored displacement values from (a) 01-8-3 to 01-9-2, (b) 01-9-14 to 01-11-5, (c) 01-11-16 to 01-12-14, (d) 02-1-2 to 02-3-2, (e) 02-3-11 to 02-3-31 for inclinometer borehole cx9 at No.2 Bachimen landslide, Funing expressway, Fujian, the data series for A or B direction at each point with 1 m depth intervals were used to build the corresponding SVMs.

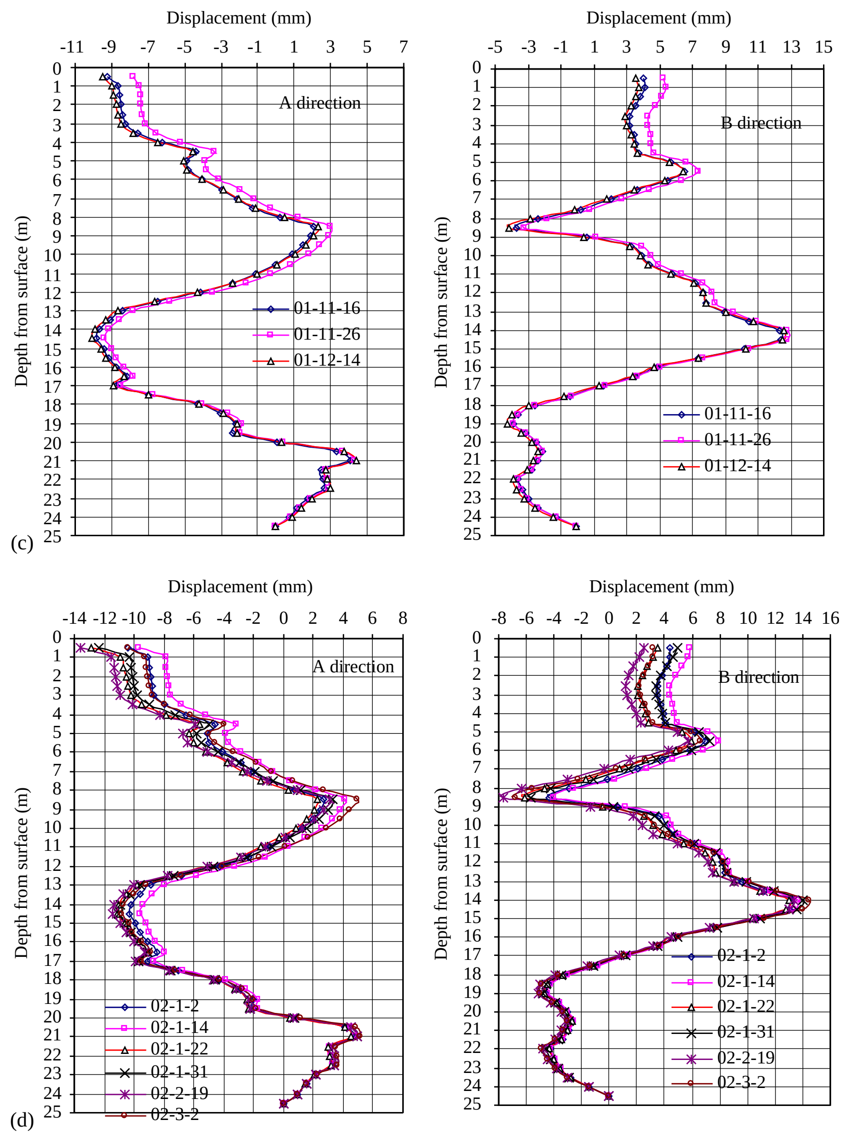

Fig. 9 (*continued*).

3.2. Evolutionary SVMs

An evolutionary SVM uses a genetic algorithm to search the kernel function and its training parameters with the input of the training sample set. The tentative SVMs are tested by the testing sample set. The training process of the SVMs will be completed when the identified SVMs can give good generalized predictions for testing samples. The algorithm can be summarized as follows:

Step 1: Collect a set of a monitored displacement time series to construct a training SVM sample set. A testing sample set is built by selecting randomly from the monitored displacement time series, which may not be included in the training sample set.

Step 2: Initialize parameters for evolution such as the number of evolutionary generations, population size, creep mutation probability, jump mutation probability, range of the kernel function and its parameters including b, C and σ.

Step 3: Select randomly a kernel function from common examples of kernel functions such as polynomials, Gaussian radial base, and Sigmoid. Produce randomly a set of C, b and σ in the given ranges. Every created kernel function and its parameters such as C, b and σ is regarded as an individual of the tentative SVMs.

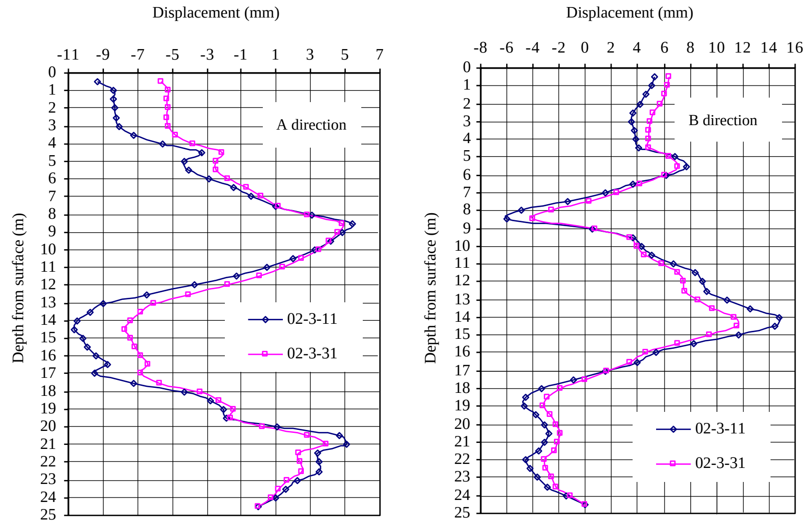

(e)

Fig. 9 (*continued*).

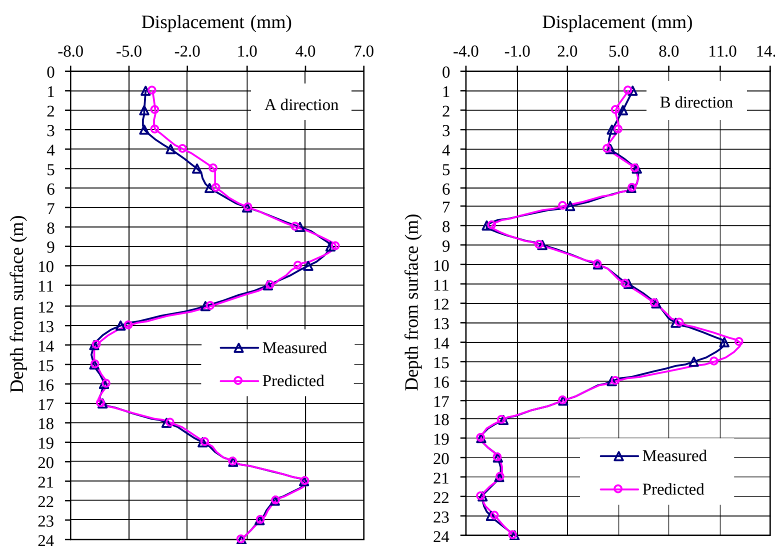

Fig. 10. Comparison of displacements monitored and predicted by the SVMs for each point with 1 m interval along depth of borehole cx9 for No.2 landslide on 11 May 2002, the data were not used to build the SVMs.

Step 4: Use the SMO algorithm to solve the quadratic programming problems, including every tentative SVM individual, to obtain their support vectors.

Step 5: The selected parameters and the obtained support vectors represent a SVM model. Use the testing samples to test the prediction ability of the SVM models. The applicability of the model is indicated by fitness:

$$fitness = \max\left(\left\{\frac{|x_i - \hat{x}_i|}{x_i}\right\}, i = 1, 2, \ldots, q\right), \qquad (11)$$

where $x_i, \hat{x}_i$ are the measured and predicted displacements for output of the ith testing sample series. q is the number of the testing samples.

Step 6: If fitness is accepted then the training procedure of the SVMs is completed. Otherwise, select randomly two individuals i_1, i_2 whose fitnesses are less than the average value to perform a crossover operation to create two new SVM individuals.

Step 7: One of the new individual SVMs is mutated using the creep mutation probability and jump mutation probability to produce a new individual.

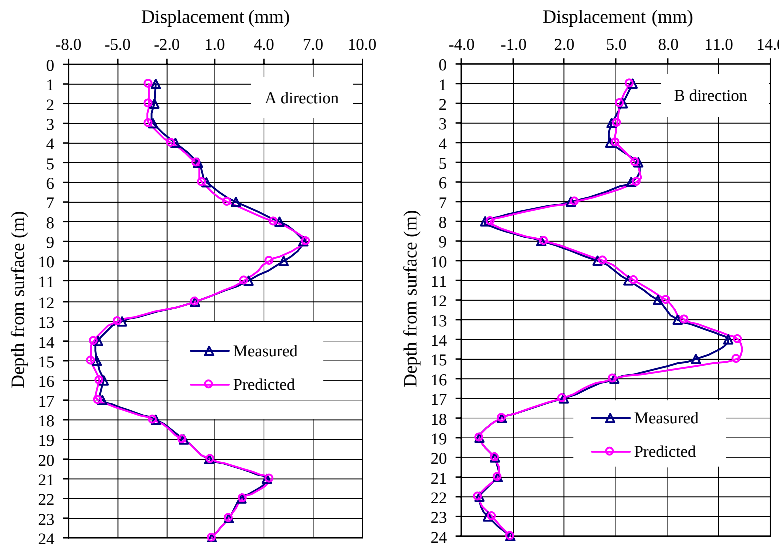

Fig. 11. Comparison of displacements monitored and predicted by the SVMs for each point at 1 m depth intervals of borehole cx9 for No.2 landslide on 21 May 2002, the data were not used to build the SVMs.

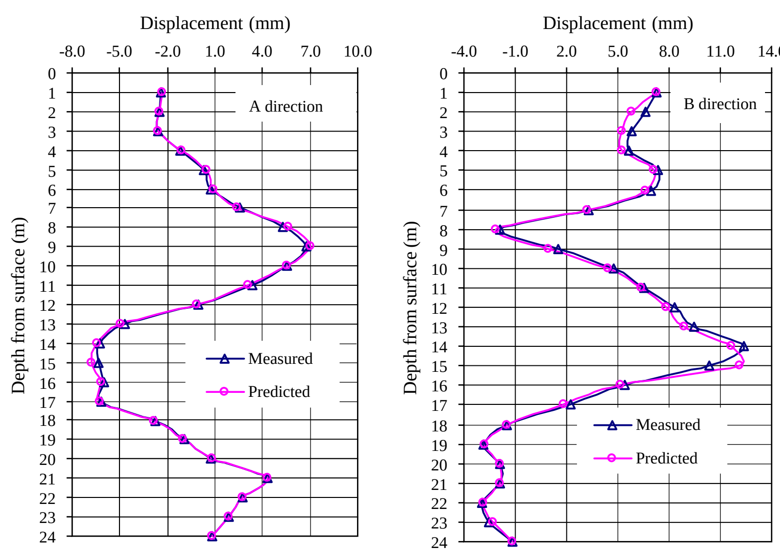

Fig. 12. Comparison of displacements monitored and predicted by the SVMs at each point for 1 m depth intervals of borehole cx9 for No.2 landslide on 31 May 2002, the data were not used to build the SVMs.

Step 8: If all new individuals of population size are generated, then go to Step 4; otherwise, go to Step 6.

3.3. Prediction of generalization

If a SVM is established for a non-linear displacement time series $\{x_t\} = (x_1, x_2, \ldots, x_n)$, then it can be used to predict the future displacements of the time series by iteration. The basic idea is as follows. First, the displacement $\hat{x}_{n+1}$ at time step $n+1$ is predicted by using the SVM model for the input vector $(x_{n-p+1}, \ldots, x_n)$. Then, the predicted $\hat{x}_{n+1}$ can be added to the input vector and the displacement at the previous time step n–$P+1$ is deleted so that the input vector has the same time steps as before. The updated input vector is used to predict the displacement $\hat{x}_{n+2}$ for the next time step $n+2$. In turn, the new predicted displacement $\hat{x}_{n+2}$

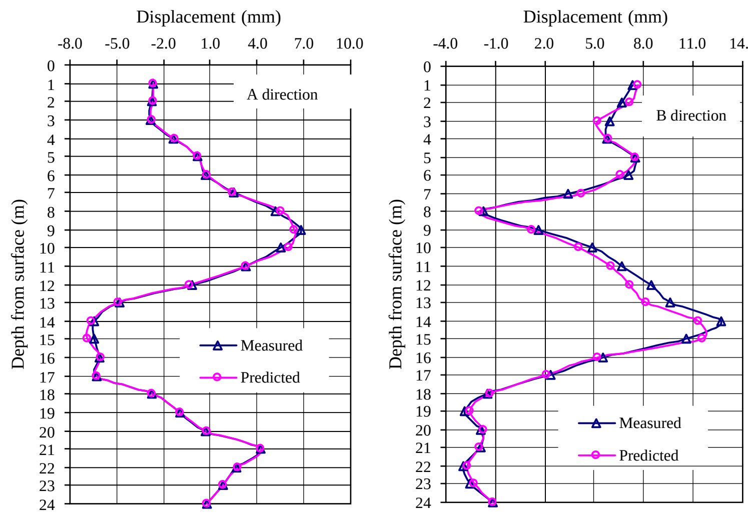

Fig. 13. Comparison of displacements monitored and predicted by the SVMs for each point for 1 m depth intervals of borehole cx9 for no.2 landslide on 10 June 2002, the data were not used to build the SVMs.

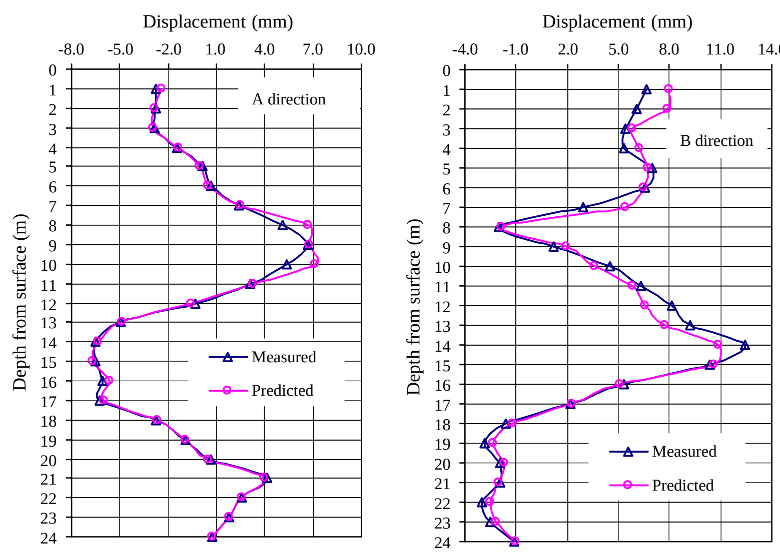

Fig. 14. Comparison of displacements monitored and predicted by the SVMs for each point for 1 m depth intervals of borehole cx9 at No.2 landslide on 21 June 2002, the data were not used to build the SVMs.

is then used to update the input vector for predicting the displacement at time step $n+3$. The loop is finished when the displacement $\hat{x}_{n+m}$ at the expected time step $n+m$ is appropriately predicted.

Normally, the accuracy of prediction decreases with the increase of time steps. Therefore, a multi-stage prediction model is necessary for longer time series in prediction to obtain acceptable accuracy. For multi-stage prediction modeling, continuous displacement measurement is necessary. At each stage, the measured displacement values are used to train the SVM model and predict the behavior for multi-time steps.

4. Case studies

4.1. *Study of non-linear displacement time series for the slope at the permanent shiplock, Three Gorges Project, China*

The permanent shiplock of the Three Gorges Project is located on the right bank of the Yangtze river in China (Fig. 1). The normal height of the slope is 100–160 m with a maximum height of 170 m. After completion of the slope excavation, its long-term deformation will directly affect the function and operational safety of

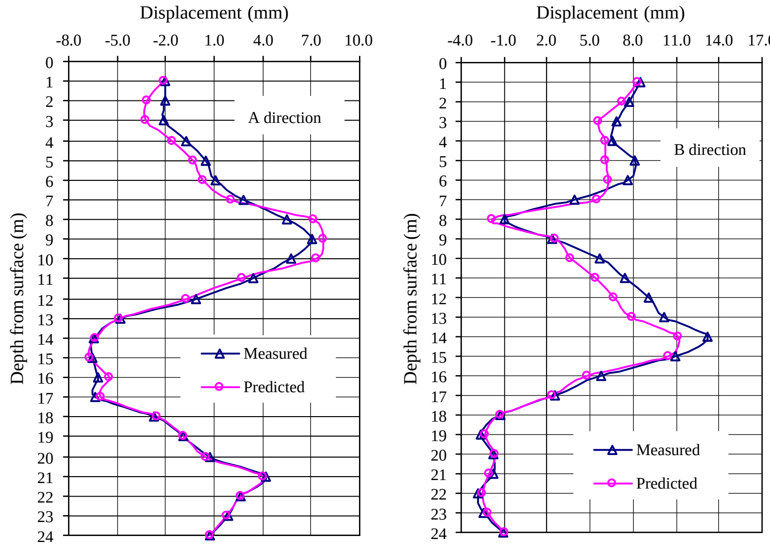

Fig. 15. Comparison of displacements monitored and predicted by the SVMs for each point for 1 m depth intervals of borehole cx9 for No.2 landslide on 1 July 2002, the data were not used to build the SVMs.

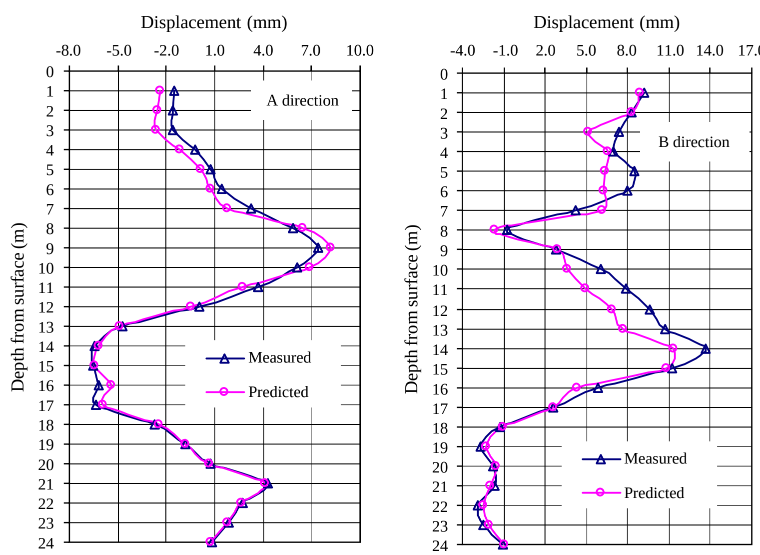

Fig. 16. Comparison of displacements monitored and predicted by the SVMs for each point for 1 m depth intervals of borehole cx9 for No.2 landslide on 11 July 2002, the data were not used to build the SVMs.

the shiplock and other nearby facilities. The safety monitoring has being conducted for better understanding of the behavior of the high shiplock slope during both excavation and operational periods. Deformations at the four measuring points, namely TP/BM11GP01, TP/BM26GP02, TP/BM27GP02, and TP/BM29GP02 of the third shiplock head (Section 17-17, the most complex section, Fig. 2) were investigated by using the evolutionary SVMs. In the SVM training, the kernel function such as polynomials, Gaussian radial base, and Sigmoid, is randomly selected; the range of the parameter C is set to be 1–5000, σ, b or d is set to be 1–300. The number of historical time steps p is taken to be six and the time step is taken to be 1 month. After evolution of 50 generations, the best SVM model with best parameters C, σ, b (shown in Table 1) and the best support vectors (shown in Table 2) are found. With the recognized SVMs, the displacements for the future 10 time steps (months) are predicted (Figs. 3–6). With the accuracy of model generalization being considered,

Table 3
Parameter values of SVM models for monitoring borehole cx9, Bachimen landslide, Fujian, China

Depth from surface (m)	*A* direction			*B* direction		
	C	σ	*b*	*C*	σ	*b*
1	210	40	−3.54	272	30	2.18
2	111	34	−3.77	424	29	1.43
3	226	39	−2.88	907	26	1.14
4	484	34	−1.69	528	49	1.91
5	569	74	−1.23	252	12	2.82
6	752	33	0.47	790	48	2.79
7	64	9	1.19	766	37	1.21
8	439	6	0.06	84	48	−2.20
9	697	13	1.43	457	30	−0.34
10	868	9	0.93	142	14	1.77
11	733	31	−0.40	677	20	2.39
12	784	21	−1.48	491	46	3.08
13	1	26	−4.88	454	39	4.04
14	272	40	−2.96	886	11	5.04
15	210	38	−2.77	305	19	4.32
16	81	27	−3.14	194	8	2.51
17	106	27	−3.24	910	8	1.48
18	153	25	−1.54	379	30	−1.05
19	117	27	−0.85	109	34	−1.70
20	993	36	−0.22	565	49	−0.91
21	337	32	1.51	809	36	−1.05
22	500	31	0.90	369	50	−1.62
23	825	35	0.70	789	36	−1.33
24	387	22	0.33	275	14	−0.46

two-stage modeling is adopted for the displacement predictions of the monitoring points TP/BM11GP01, TP/BM26GP02, and TP/BM27GP02 and three-stage modeling for that of the point TP/BM29GP02.

4.2. Study of non-linear displacement time series for the Bachimen landslide, Fujian, China

The Bachimen landslide is located in the area of Maping and Guojing, Fujian province (Fig. 1). With the acceleration of the Funing expressway construction, the landslide hazard becomes more significant. In June 2000, due to a continuous storm, the underground water table was elevated, the soil pore pressure on the sliding face was increased, the soil strength was decreased, and the sliding resistance was decreased with the pipe surging effect in soil strengthened while the sliding force was increased. In addition, because of the route change in the lower part of an ancient landslide, the engineering construction damaged the natural slope of the ancient landslide and destroyed the natural stress balance in the slope. This caused a change in the expressway route locally. There occurred sliding and cracking in the mountain slope between BCK0 + 400 ~ 450. The maximum crack opening was 1.6 m with expressway surface subsidence of 1.5 m.

4.2.1. Geological and hydro-geological conditions

The Bachimen landslide strata are mainly clastic soil, rubbishy tuff, and locally tuff. The hydro-geological conditions in the landslide are complex. The surface is not abundant in water, while the underground is rich in water, and there are two underground aquifers. The first aquifer is comprised of loose clay with high porosity and permeability. According to the pumping tests at boreholes ZK22, ZK26 and ZK35, the water flow is 24, 5.2 and 1.3 m^3/day, respectively. The supplementary source is atmospheric precipitation, with the overland flow direction controlled by surface topography. Drainage is mainly due to surface evaporation. The second aquifer is also clay and its lower layers contain underground water at low pressure. Its supplementary source is the perpendicular infiltration of atmospheric precipitation. Drainage is in the form of spring mouths with the water flow of the spring mouths being 0.01–2.2 l/s.

4.2.2. Monitoring of landslide

We have conducted sliding slope monitoring, including ground surface displacement monitoring, sliding body displacement monitoring at depth, monitoring of water table and cable force, monitoring of anti-sliding pile resistance and displacement. The layout of the measuring points is shown in Fig. 7. There are 50 monitoring boreholes in total with measuring pipes to monitor the slope sliding deformation at the depth. At 1.0 m intervals of borehole depth, measured evolutionary displacement series in two directions were obtained. For instance, the measured results of displacement evolutions in the two directions of *A* and *B* (their azimuths are NE13 and SW103 respectively) of cx9 borehole on the landslide are shown in Fig. 8.

The measured in situ displacement time series is used to establish the SVMs and to predict the future displacement behaviour. This paper presents the results of the displacement prediction results at inclinometer borehole cx9, instrumented for monitoring the No.2 landslide. The borehole is 25 m in depth (Fig. 8). Fourty eight non-linear displacement time series SVMs in total were obtained, one for the displacement time series of the directions *A* or *B* at each monitoring point arranged at depth intervals of one meter from ground surface. The SVM models were established by using the monitored displacement in the period from 3 August, 2001 to 31 March 2002 (Fig. 9) and were used to predict displacements for the period from April 11 to July 11 2002. The results are shown in Figs. 10–16. The time step interval is set to about 10 days. The SVM model shown in Tables 3 and 4 is trained at ranges of 1–1000, 1–100, 1–100 for the parameters *C*, σ and *b*, historical time point *p* (= 5), population size (50), kernel

Table 4
Values of Lagrange multipliers of SVMs for monitoring borehole cx9, Bachimen landslide, Fujian, China

Depth (m)	Direction		No. of learning samples																			
			1	2	3	**4**	5	6	7	8	9	10	11	12	13	14	15	16	17	18	19	20
1	*A*	α	210.00	0.00	0.00	0.00	0.00	0.00	152.81	0.00	0.00	0.00	0.00	3.19	0.00	0.00	0.00	0.00	0.00	0.00	17.36	210.00
		α*	0.00	130.16	20.31	32.83	44.06	0.00	0.00	152.81	0.00	0.00	0.00	0.00	3.19	0.00	0.00	210.00	0.00	0.00	0.00	0.00
	B	α	0.00	0.00	59.25	0.00	123.54	272.00	0.00	0.00	0.00	272.00	0.00	272.00	0.00	0.00	0.00	0.00	0.00	138.07	5.15	0.00
		α*	45.38	30.21	0.00	130.60	0.00	0.00	189.36	59.25	272.00	0.00	0.00	0.00	0.00	0.00	0.00	272.00	143.21	0.00	0.00	0.00
2	*A*	α	111.00	0.00	13.80	0.00	0.00	0.00	0.00	0.00	0.00	0.00	0.00	0.00	0.00	0.00	0.00	0.00	0.00	0.00	0.00	111.00
		α*	0.00	48.44	0.00	62.56	13.80	0.00	0.00	0.00	0.00	0.00	0.00	0.00	0.00	0.00	0.00	111.00	0.00	0.00	0.00	0.00
	B	α	34.11	0.00	241.97	0.00	140.62	141.10	348.68	130.05	0.00	156.68	83.07	368.60	0.00	0.00	0.00	0.00	0.00	424.00	232.71	424.00
		α*	0.00	376.04	0.00	216.62	0.00	0.00	0.00	0.00	424.00	0.00	0.00	0.00	424.00	12.93	424.00	424.00	424.00	0.00	0.00	0.00
3	*A*	α	226.00	0.00	0.00	0.00	0.00	0.00	201.21	0.00	0.00	0.00	0.00	62.19	0.00	0.00	0.00	0.00	0.00	0.00	24.82	226.00
		α*	0.00	92.56	74.75	4.39	79.21	0.00	0.00	201.21	0.00	0.00	0.00	0.00	62.19	0.00	0.00	226.00	0.00	0.00	0.00	0.00
	B	α	179.81	0.00	708.39	0.00	369.15	218.79	334.47	143.42	0.00	907.00	608.53	310.33	0.00	157.44	0.00	0.00	0.00	795.84	907.00	265.28
		α*	0.00	876.17	0.00	494.29	0.00	0.00	0.00	0.00	907.00	0.00	0.00	0.00	907.00	0.00	907.00	907.00	907.00	0.00	0.00	0.00
4	*A*	α	484.00	0.00	0.00	237.49	0.00	0.00	427.23	0.00	254.44	0.00	0.00	484.00	0.00	0.00	0.00	0.00	347.85	0.00	228.84	169.59
		α*	0.00	223.50	2.74	0.00	439.88	453.96	0.00	81.60	0.00	27.81	17.73	0.00	376.09	362.29	14.55	446.65	0.00	186.63	0.00	0.00
	B	α	0.00	0.00	267.41	0.00	345.44	37.78	506.58	374.36	0.00	0.00	0.00	528.00	0.00	327.17	0.00	0.00	0.00	528.00	378.08	528.00
		α*	138.73	343.26	0.00	353.57	0.00	0.00	0.00	0.00	528.00	308.52	89.29	0.00	528.00	0.00	475.46	528.00	528.00	0.00	0.00	0.00
5	*A*	α	569.00	569.00	0.00	0.00	0.00	0.00	569.00	569.00	0.00	363.36	94.96	0.00	0.00	351.10	78.92	0.00	258.88	0.00	0.00	569.00
		α*	0.00	0.00	569.00	9.23	569.00	569.00	0.00	0.00	569.00	0.00	0.00	0.00	569.00	0.00	0.00	569.00	0.00	569.00	0.00	0.00
	B	α	0.00	5.40	19.73	0.00	0.00	0.00	15.98	0.00	0.00	3.39	5.59	252.00	0.00	27.18	0.00	0.00	0.00	25.42	0.00	0.00
		α*	15.54	0.00	0.00	4.59	18.96	17.14	0.00	7.00	12.09	0.00	0.00	0.00	29.71	0.00	9.07	186.42	50.98	0.00	0.81	2.39
6	*A*	α	752.00	0.00	178.54	0.00	0.00	0.00	752.00	0.00	49.13	29.55	2.20	126.15	0.00	0.00	0.00	38.87	73.85	0.00	67.22	51.85
		α*	0.00	199.49	0.00	79.22	345.90	735.84	0.00	203.66	0.00	0.00	0.00	0.00	213.12	250.15	85.82	0.00	0.00	8.16	0.00	0.00
	B	α	0.00	64.85	700.89	0.00	0.00	0.00	164.93	0.00	0.00	33.53	57.63	790.00	0.00	161.44	0.00	0.00	90.70	256.98	27.48	15.41
		α*	350.00	0.00	0.00	308.79	95.28	218.11	0.00	117.30	89.53	0.00	0.00	0.00	250.19	0.00	144.64	790.00	0.00	0.00	0.00	0.00
7	*A*	α	64.00	0.00	8.64	21.56	0.00	0.00	64.00	0.00	0.00	0.46	22.40	54.94	42.91	0.00	5.35	13.29	17.37	0.00	34.79	0.26
		α*	0.00	23.57	0.00	0.00	6.37	64.00	0.00	64.00	64.00	0.00	0.00	0.00	0.00	64.00	0.00	0.00	0.00	64.00	0.00	0.00
	B	α	0.00	179.80	443.25	0.00	766.00	0.00	740.98	576.87	0.00	0.00	0.00	337.84	49.19	0.00	148.51	0.00	195.77	0.00	471.95	61.44
		α*	187.31	0.00	0.00	766.00	0.00	766.00	0.00	0.00	766.00	0.00	0.00	0.00	0.00	87.57	0.00	666.25	0.00	732.47	0.00	0.00
8	*A*	α	30.99	0.00	0.00	97.03	32.43	0.00	77.14	0.00	28.31	0.00	0.00	439.00	0.00	67.04	107.79	0.00	249.44	439.00	87.28	71.55
		α*	0.00	145.58	205.71	0.00	0.00	74.84	0.00	388.12	0.00	224.24	87.00	0.00	358.81	0.00	0.00	242.72	0.00	0.00	0.00	0.00
	B	α	74.33	84.00	0.00	0.00	84.00	9.67	0.00	0.00	0.00	0.00	0.00	0.00	0.00	0.00	0.00	0.00	0.00	0.00	0.00	0.00
		α*	0.00	0.00	84.00	84.00	0.00	0.00	0.00	0.00	0.00	0.00	0.00	0.00	0.00	0.00	0.00	84.00	0.00	0.00	0.00	0.00
9	*A*	α	0.00	99.12	0.00	0.00	103.41	0.00	605.86	0.00	0.00	0.00	29.96	610.01	0.00	60.32	90.72	0.00	0.00	697.00	89.28	0.00
		α*	19.09	0.00	224.21	123.34	0.00	249.46	0.00	148.10	159.38	601.46	0.00	0.00	577.31	0.00	0.00	222.91	0.00	0.00	0.00	60.42
	B	α	0.00	95.59	0.00	0.00	0.00	0.00	284.64	402.54	0.00	457.00	457.00	457.00	0.00	457.00	0.00	0.00	0.00	0.00	0.00	0.00
		α*	0.00	0.00	5.94	23.58	40.59	457.00	0.00	0.00	457.00	0.00	0.00	0.00	457.00	0.00	404.70	457.00	307.97	0.00	0.00	0.00
10	*A*	α	198.34	0.00	0.00	108.63	284.05	0.00	225.69	0.00	0.00	133.24	0.00	844.49	0.00	0.00	0.00	0.00	560.74	868.00	868.00	512.91
		α*	0.00	868.00	641.05	0.00	0.00	584.00	0.00	868.00	103.58	0.00	306.73	0.00	868.00	25.86	73.09	274.55	0.00	0.00	0.00	0.00
	B	α	0.00	13.39	15.68	7.47	25.22	0.00	99.56	0.00	0.00	2.82	142.00	104.12	0.00	56.10	0.00	0.00	25.64	30.23	49.01	5.52
		α*	34.95	0.00	0.00	0.00	0.00	142.00	0.00	74.83	34.73	0.00	0.00	0.00	104.08	0.00	44.19	142.00	0.00	0.00	0.00	0.00
11	*A*	α	733.00	80.29	0.00	709.68	0.00	0.00	605.55	75.80	0.00	733.00	733.00	584.97	0.00	0.00	0.00	0.00	711.25	0.00	733.00	733.00
		α*	0.00	0.00	733.00	0.00	568.55	733.00	0.00	0.00	733.00	0.00	0.00	0.00	733.00	733.00	733.00	733.00	0.00	733.00	0.00	0.00
	B	α	0.00	16.18	0.00	0.00	341.70	0.00	677.00	0.00	0.00	443.68	0.00	677.00	0.00	138.46	0.00	0.00	55.91	677.00	472.05	440.75
		α*	37.39	0.00	52.30	310.90	0.00	566.96	0.00	422.28	677.00	0.00	2.82	0.00	677.00	0.00	677.00	516.07	0.00	0.00	0.00	0.00
12	*A*	α	784.00	0.00	389.79	0.00	0.00	0.00	784.00	0.00	400.45	113.50	384.53	784.00	0.00	0.00	0.00	0.00	555.90	0.00	398.33	421.58
		α*	0.00	631.43	0.00	170.97	126.71	638.24	0.00	784.00	0.00	0.00	0.00	0.00	651.59	477.61	571.56	784.00	0.00	179.98	0.00	0.00
	B	α	0.00	47.45	69.78	5.71	491.00	0.00	491.00	0.00	0.00	44.80	84.26	491.00	353.72	376.93	0.00	0.00	491.00	491.00	0.00	0.00
		α*	208.03	0.00	0.00	0.00	0.00	491.00	0.00	491.00	491.00	0.00	0.00	0.00	0.00	0.00	491.00	491.00	0.00	0.00	283.62	491.00

Table 4 (*continued*)

Depth (m)	Direction		No. of learning samples																			
			1	2	3	**4**	5	6	7	8	9	10	11	12	13	14	15	16	17	18	19	20
13	*A*	α	1.00	1.00	0.00	0.00	0.00	0.00	0.00	0.00	0.00	0.00	0.00	0.00	0.00	0.00	0.00	0.00	0.00	0.00	0.00	0.00
		α^*	0.00	0.00	1.00	0.00	0.00	0.00	0.00	0.00	0.00	0.00	0.00	0.00	0.00	0.00	0.00	1.00	0.00	0.00	0.00	0.00
	B	α	99.88	0.00	0.00	58.49	454.00	0.00	454.00	0.00	0.00	326.58	454.00	454.00	0.00	454.00	0.00	0.00	454.00	454.00	0.00	0.00
		α^*	0.00	313.76	205.72	0.00	0.00	304.90	0.00	282.05	454.00	0.00	0.00	0.00	454.00	0.00	454.00	454.00	0.00	0.00	286.52	454.00
14	*A*	α	272.00	0.00	215.75	0.00	0.00	0.00	67.54	0.00	21.11	1.74	6.76	13.34	0.00	11.21	0.00	3.21	0.00	14.78	26.71	258.75
		α^*	0.00	197.91	0.00	253.09	73.95	68.18	0.00	10.31	0.00	0.00	0.00	0.00	25.43	0.00	12.04	0.00	272.00	0.00	0.00	0.00
	B	α	0.00	0.00	0.00	22.09	90.00	44.40	90.00	0.00	0.00	33.76	41.57	66.86	0.00	90.00	0.00	0.00	79.37	41.40	0.00	0.00
		α^*	0.00	90.00	60.21	0.00	0.00	0.00	0.00	90.00	40.84	0.00	0.00	0.00	90.00	0.00	37.95	10.45	0.00	0.00	90.00	90.00
15	*A*	α	210.00	0.00	205.14	0.00	0.00	0.00	36.51	11.46	0.00	1.36	6.39	10.42	0.00	6.34	0.00	1.13	5.56	6.90	0.00	48.30
		α^*	0.00	158.83	0.00	35.77	91.13	210.00	0.00	0.00	2.75	0.00	0.00	0.00	19.40	0.00	6.91	0.00	0.00	0.00	24.72	0.00
	B	α	0.00	0.00	0.00	18.60	63.59	43.15	67.03	0.00	0.00	32.33	0.00	305.00	0.00	79.65	305.00	0.00	74.41	48.91	0.00	0.00
		α^*	0.00	63.27	24.61	0.00	0.00	0.00	0.00	157.88	13.07	0.00	32.09	0.00	305.00	0.00	0.00	58.51	0.00	0.00	90.14	293.10
16	*A*	α	81.00	0.00	66.79	0.00	0.00	0.00	7.01	2.25	1.94	0.63	1.05	0.00	0.00	1.73	0.00	0.53	2.32	1.05	8.65	13.85
		α^*	0.00	60.91	0.00	75.91	26.73	0.00	0.00	0.00	0.00	0.00	0.00	20.85	2.83	0.00	1.55	0.00	0.00	0.00	0.00	0.00
	B	α	15.94	0.00	0.00	20.56	160.36	0.00	194.00	0.00	0.00	12.13	7.40	194.00	0.00	194.00	0.00	0.00	102.43	194.00	102.23	0.00
		α^*	0.00	54.76	61.06	0.00	0.00	61.47	0.00	49.76	194.00	0.00	0.00	0.00	194.00	0.00	194.00	194.00	0.00	0.00	0.00	194.00
17	*A*	α	106.00	0.00	89.64	0.00	0.00	0.00	20.53	0.00	9.31	0.23	2.84	7.08	0.00	2.24	0.00	0.00	5.51	2.20	17.02	86.84
		α^*	0.00	93.68	0.00	89.12	29.60	14.03	0.00	1.29	0.00	0.00	0.00	0.00	12.88	0.00	2.84	106.00	0.00	0.00	0.00	0.00
	B	α	0.00	619.68	762.82	0.00	13.76	0.00	488.75	618.97	0.00	219.74	0.00	390.77	0.00	192.15	0.00	0.00	476.28	656.60	0.00	0.00
		α^*	321.39	0.00	0.00	296.79	0.00	910.00	0.00	0.00	504.44	0.00	477.78	0.00	417.47	0.00	910.00	303.94	0.00	0.00	271.66	26.05
18	*A*	α	153.00	0.00	68.28	0.00	0.00	0.00	21.67	6.88	0.00	4.89	2.04	14.16	0.00	4.82	0.00	0.76	0.00	12.69	17.99	19.25
		α^*	0.00	128.30	0.00	81.54	41.80	13.29	0.00	0.00	2.88	0.00	0.00	0.00	23.66	0.00	3.39	0.00	31.55	0.00	0.00	0.00
	B	α	379.00	0.00	0.00	142.97	379.00	0.00	0.00	0.00	366.82	356.10	0.00	379.00	0.00	136.90	0.00	0.00	379.00	0.00	130.65	66.08
		α^*	0.00	241.31	76.56	0.00	0.00	379.00	379.00	192.31	0.00	0.00	242.23	0.00	379.00	0.00	379.00	379.00	0.00	68.11	0.00	0.00
19	*A*	α	117.00	0.00	43.64	0.00	0.00	0.00	9.25	0.00	0.00	9.79	11.14	21.23	0.00	0.00	0.00	0.00	25.53	13.70	0.95	34.03
		α^*	0.00	102.05	0.00	19.66	23.98	0.00	0.00	2.30	6.95	0.00	0.00	0.00	42.16	0.00	89.17	0.00	0.00	0.00	0.00	0.00
	B	α	109.00	109.00	0.00	0.00	0.00	0.00	0.00	0.00	0.00	0.00	0.00	0.00	0.00	0.00	0.00	0.00	0.00	0.00	15.00	0.00
		α^*	0.00	0.00	65.80	58.20	0.00	0.00	0.00	109.00	0.00	0.00	0.00	0.00	0.00	0.00	0.00	0.00	0.00	0.00	0.00	0.00
20	*A*	α	0.00	0.00	0.00	698.48	993.00	659.14	993.00	219.94	0.00	112.50	712.04	311.14	0.00	0.00	0.00	0.00	993.00	819.44	993.00	0.00
		α^*	993.00	993.00	948.49	0.00	0.00	0.00	0.00	0.00	993.00	0.00	0.00	0.00	993.00	10.80	993.00	993.00	0.00	0.00	0.00	587.40
	B	α	565.00	0.00	0.00	0.00	0.00	0.00	0.00	0.00	0.00	32.39	38.17	11.96	0.00	0.00	0.00	0.00	17.65	27.18	235.74	0.00
		α^*	0.00	28.83	0.00	0.00	0.00	235.74	0.00	0.00	536.17	0.00	0.00	0.00	1.70	0.00	4.18	2.32	0.00	0.00	0.00	119.15
21	*A*	α	0.00	228.71	0.00	50.77	173.23	93.14	0.00	0.00	0.00	0.80	7.99	0.00	337.00	4.15	0.00	4.11	6.25	0.00	0.00	0.00
		α^*	337.00	0.00	89.46	0.00	0.00	0.00	33.97	24.73	32.13	0.00	0.00	2.34	0.00	0.00	9.70	0.00	0.00	2.31	53.07	321.42
	B	α	809.00	0.00	0.00	0.00	0.00	0.00	0.00	0.00	0.00	0.00	0.00	10.82	5.88	0.00	0.15	0.00	0.00	22.85	25.53	158.77
		α^*	0.00	86.46	0.00	0.00	0.00	809.00	0.00	0.00	0.00	0.00	0.00	0.00	0.00	5.05	0.00	1.03	131.47	0.00	0.00	0.00
22	*A*	α	0.00	408.92	0.00	54.19	180.80	57.39	0.00	0.00	0.00	0.00	1.62	0.00	500.00	1.67	0.00	0.00	1.29	0.00	0.00	0.00
		α^*	500.00	0.00	134.19	0.00	0.00	0.00	40.45	24.46	27.85	0.87	0.00	5.42	0.00	0.00	3.84	0.08	0.00	3.06	36.42	429.23
	B	α	369.00	369.00	0.00	0.00	0.00	0.00	0.00	0.00	0.00	0.00	0.00	0.00	0.00	0.00	0.00	0.00	0.00	0.00	3.49	0.00
		α^*	0.00	0.00	321.40	51.09	0.00	369.00	0.00	0.00	0.00	0.00	0.00	0.00	0.00	0.00	0.00	0.00	0.00	0.00	0.00	0.00
23	*A*	α	0.00	350.86	0.00	85.93	194.90	128.20	825.00	0.00	0.00	0.00	0.00	0.00	0.00	19.67	0.00	0.00	26.38	0.00	0.00	0.00
		α^*	825.00	0.00	200.69	0.00	0.00	0.00	0.00	104.54	47.97	4.64	3.76	20.63	43.35	0.00	16.92	6.45	0.00	11.18	266.38	79.44
	B	α	789.00	0.00	789.00	0.00	199.26	0.00	442.47	32.01	40.96	1.49	13.58	704.68	0.00	0.94	0.18	1.49	0.00	0.00	789.00	789.00
		α^*	0.00	648.05	0.00	789.00	0.00	789.00	0.00	0.00	0.00	0.00	0.00	0.00	789.00	0.00	0.00	0.00	789.00	789.00	0.00	0.00
24	*A*	α	275.00	0.00	275.00	0.00	0.00	0.00	0.00	0.00	5.64	5.45	5.08	3.86	1.26	2.43	0.93	1.68	0.00	0.81	22.80	0.00
		α^*	0.00	245.24	0.00	267.06	56.19	0.00	0.00	0.00	0.00	0.00	0.00	0.00	0.00	0.00	0.00	0.00	1.70	0.00	0.00	29.76
	B	α	275.00	0.00	275.00	0.00	0.00	0.00	0.00	0.00	5.64	5.45	5.08	3.86	1.26	2.43	0.93	1.68	0.00	0.81	2280	0.00
		α^*	0.00	245.24	0.00	267.06	56.19	0.00	0.00	0.00	0.00	0.00	0.00	0.00	0.00	0.00	0.00	0.00	1.70	0.00	0.00	29.76

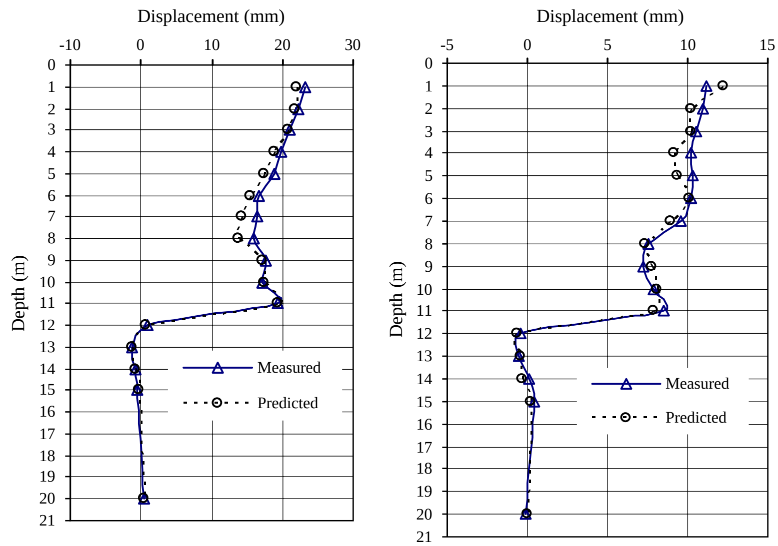

Fig. 17. Comparison of displacements monitored and predicted by the SVMs for each point for 1 m depth intervals of borehole bcx18 for landslide No.2 landslide on 30 April 2002, the SVMs were obtained using the data measured from September 13, 2001 to April 20, 2002.

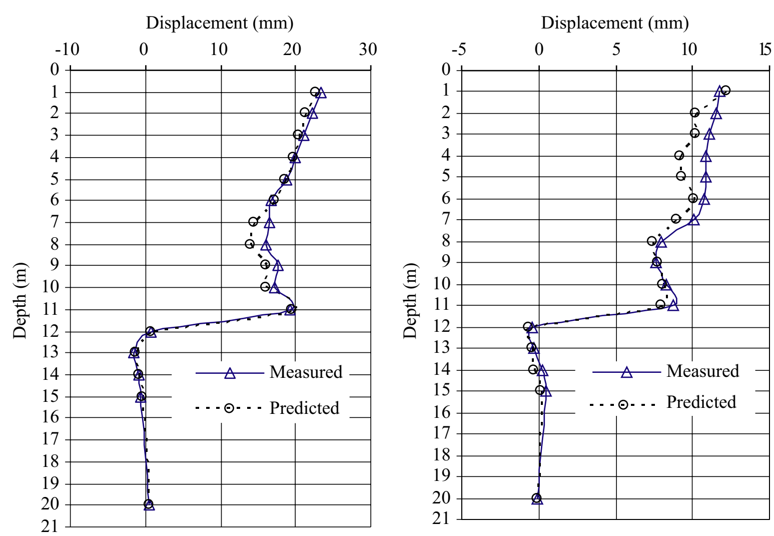

Fig. 18. Comparison of displacements monitored and predicted by the SVMs for each point for 1 m depth intervals of borehole bcx18 for landslide No.2 landslide on 10 May 2002, the SVMs were obtained using the data measured from September 13, 2001 to April 20, 2002.

function of polynomials, Gaussian radial base, and Sigmoid.

In the same way, 40 SVMs were established for non-linear displacement series at the *A* and *B* directions of the inclinometer borehole bcx18 for Landslide No.2. Figs. 17–23 show the displacement measured and predicted by the SVMs for the period of September 13, 2001 to April 20, 2002. All predictions are in good agreement with the measured results.

5. Discussions on the generalization ability of the SVMs

Using the measured displacement at previous time steps of a time series to train the tentative SVM with searching of the kernel function and its parameters in global space, the best SVM can be recognized through evolution in global space (see change of fitness of the tentative SVMs shown in Fig. 24).

The generalization ability of SVMs is related to the number of time steps for prediction (Figs. 3–6 and

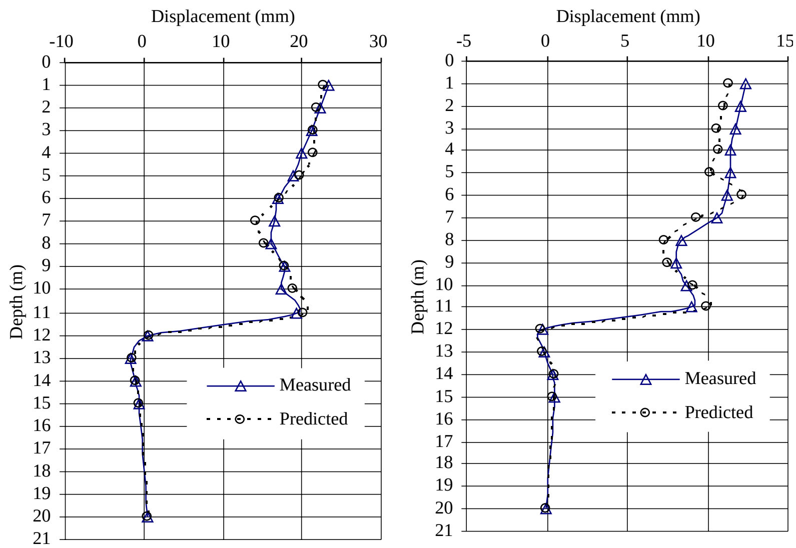

Fig. 19. Comparison of displacements monitored and predicted by the SVMs for each point for 1 m depth intervals of borehole bcx18 for landslide No.2 landslide on 20 May 2002, the SVMs were obtained using the data measured from September 13, 2001 to April 20, 2002.

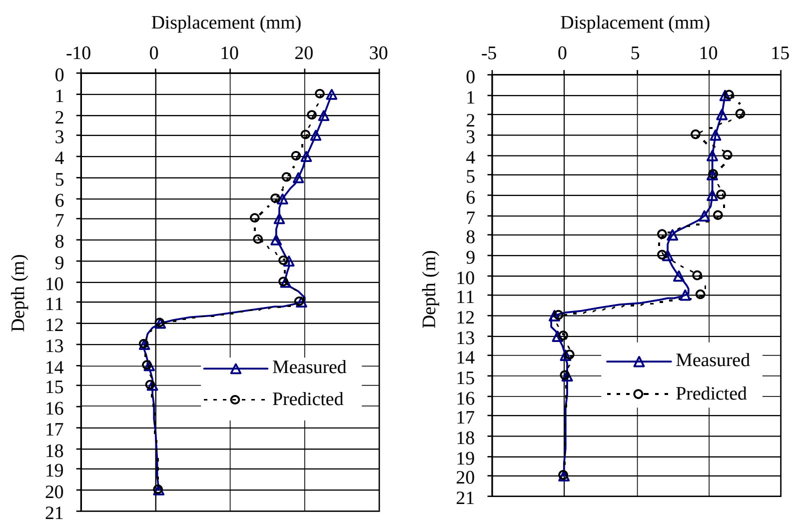

Fig. 20. Comparison of displacements monitored and predicted by the SVMs for each point for 1 m depth intervals of borehole bcx18 for landslide No.2 landslide on 30 May 2002, the SVMs were obtained using the data measured from September 13, 2001 to April 20, 2002.

10–23). When the number of time steps for prediction is small, the accuracy of prediction is high. With an increase in the number of time steps for prediction, the generalization ability of the SVMs decreases. This indicates that a suitable size of time steps needs to be established for a given problem.

However, the generalization ability of the SVMs is also controlled by the type of kernel function and its parameters. The parameter C is an important factor because the fitness of the tentative SVMs changes the value of C. There exist best SVMs having a C value with minimum fitness in all evolutionary generations for a given problem (Fig. 25). The parameter σ and d affect also generalization ability of the SVMs and the fitness of the tentative SVM changes value of σ or d. Again, there exist best SVMs having σ or d value with minimum fitness in all evolutionary generations for a given problem (Fig. 26). Therefore, a suitable algorithm is needed to recognize the best kernel function and its parameters in the global space for a given problem; otherwise, it would obtain local minimum solutions. This indicates that use of a genetic algorithm is

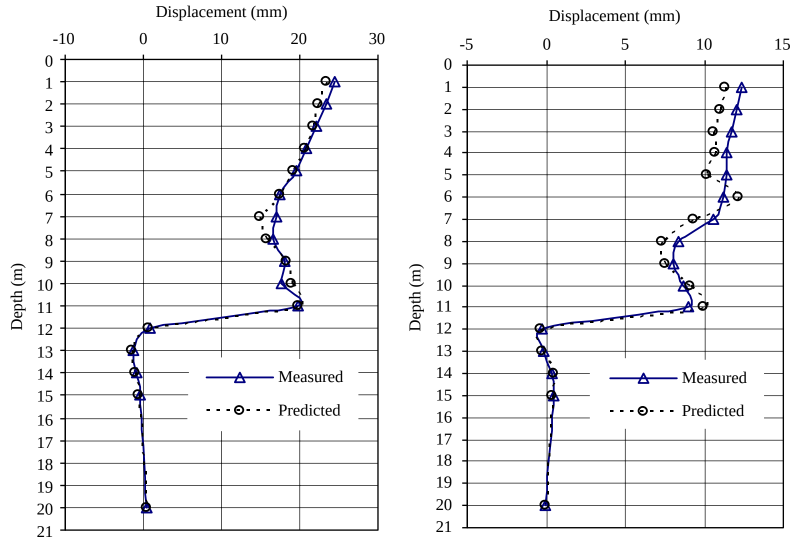

Fig. 21. Comparison of displacements monitored and predicted by the SVMs for each point for 1 m depth intervals of borehole bcx18 for landslide No.2 landslide on 9 June 2002, the SVMs were obtained using the data measured from September 13, 2001 to April 20, 2002.

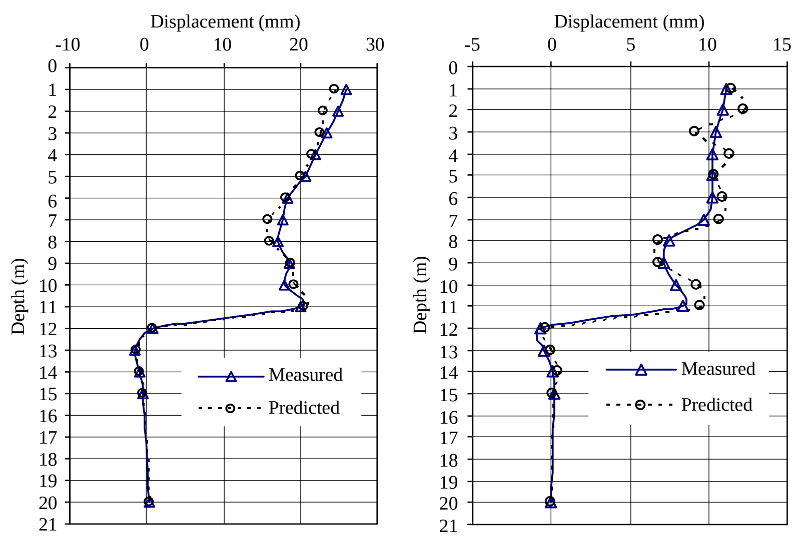

Fig. 22. Comparison of displacements monitored and predicted by the SVMs for each point for 1 m depth intervals of borehole bcx18 for landslide No.2 landslide on 19 June 2002, the SVMs were obtained using the data measured from September 13, 2001 to April 20, 2002.

attractive to obtain the global optimum SVMs for non-linear displacement time series.

6. Conclusions

The SVM is a newly developed machine learning method based on strict theoretical fundamentals. It has good adaptive capacity for solving non-linear problems with high dimensions and small samples, and has attracted attention from various research fields [18,19]. A combination of SVM and genetic algorithm is reported in this paper to formulate an evolutionary SVM algorithm for generating the time series analysis of non-linear slope deformation. Good results have been achieved also by applying the method to rock and soil engineering. Because of the complexity and high non-linearity of geo-material behavior the application of the SVM method in the geotechnical engineering field has significant potenetial.

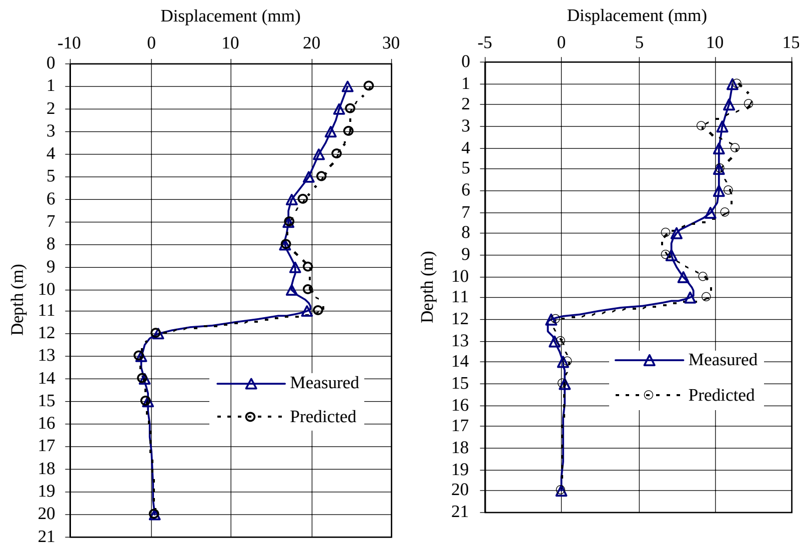

Fig. 23. Comparison of displacements monitored and predicted by the SVMs for each point for 1 m depth intervals of borehole bcx18 for landslide No.2 landslide on 7 July 2002, the SVMs were obtained using the data measured from September 13, 2001 to April 20, 2002.

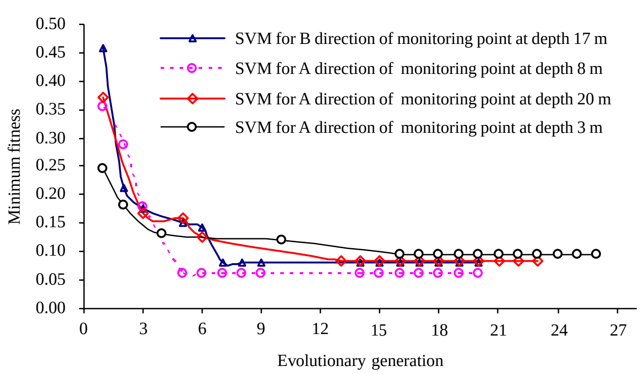

Fig. 24. Trend of the minimum fitness of tentative SVMs versus the number of evolutionary generation.

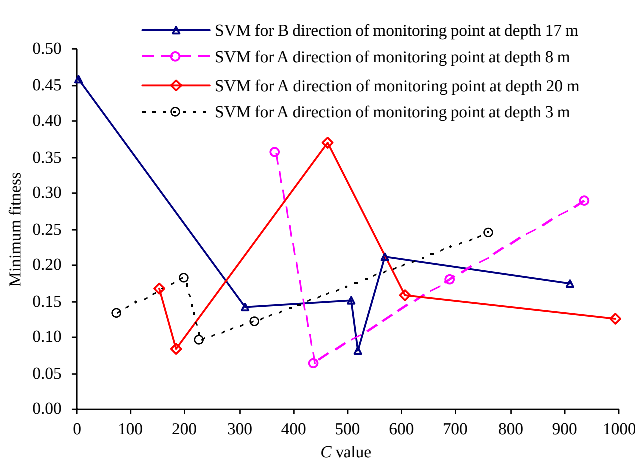

Fig. 25. Relation between the punishing factor C of support vector machines and minimum fitness of the tentative SVMs.

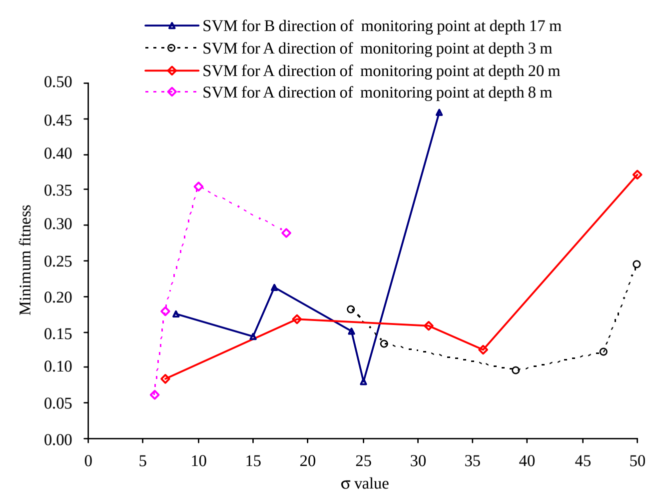

Fig. 26. Relation between the parameter σ in the kernel function of support vector machines and minimum fitness of the tentative SVMs.

Acknowledgements

Financial support from The Special Funds for Major State Basic Research Projects under Grant no. 2002CB412708 and National Natural Science Foundation of China under Grant nos. 50325414 and 50179034 are gratefully acknowledged. The authors would also like to acknowledgement Professors J.A. Hudson, Lanru Jing, and Yongjia Wang for their helpful suggestions to improve the manuscript. The Yangtze Institute of Science Research, China is thanked for assistance with the measured displacement data for four monitoring points at the Three Gorges Project, China

Special acknowledgement should also be given to Funing Expressway Ltd. Co. for their assistant on the in-situ monitoring of Bachimen Landslide.

References

[1] Feng X-T, Wang Y, Yao J. A neural network model on real-time prediction of roof pressure in coal mines. Int J Rock Mech Min Sci 1996;33(6):647–53.

[2] Feng X-T, Seto M. A new method of modeling the rock-microfracturing process in double torsion experiments using neural networks. Int J Anal Numer Meth Geomech 1999;23:905–23.

[3] Feng X-T, Seto M. Neural network dynamic modeling on rock microfracturing sequences under triaxial compressive stress condition. Tectonophysics 1998;292:293–309.

[4] Feng X-T, Seto M. Neural network dynamic modelling of acoustic emission sequences in rock. Safety Eng (Japanese) 1998;37(3):157–63.

[5] Feng X-T, Seto M, Katsuyama K. Neural dynamic modelling on earthquake magnitude series. Geophys J Int 1997;128: 547–56.

[6] Feng X-T, Zhang Z, Xu P. Adaptive and intelligent prediction of determination time series of high rock slope. Trans Nonferrous Met Soc 1999;4:842–6.

[7] Feng X-T, Katsuyama, Yongjia W, Yunmei L. A new direction—intelligent rock mechanics and rock engineering. Int J Rock Mech Min Sci 1997;34(1):135–41.

[8] Vapnik VN. The nature of statistical learning theory. New York: Springer; 1995.

[9] Vapnik VN, Golowich SE, Smola AJ. Support vector method for function approximation, regression estimation and signal processing. Adv Neural Inform Process Systems 1996;9:281–7.

[10] Scholkopf B, Burges C, Vapnik V. Extracting support data for a given task. In: Fayyad UM, Uthurusamy R, editors. Proceedings of the First International Conference on Knowledge Discovery and Data Mining. Menlo Park, CA: AAAI Press; 1995.

[11] Schmidt M. Identifying speaker with support vector networks. Interface, '96 Proceedings. Sydney, 1996.

[12] Muller KR, Smola JA, Scholkopf B. Prediction time series with support vector machines. Proceedings of International Conference on Artificial Neural Networks. Switzerland: Lausanne; 1997 p. 999–1004.

[13] Muller KR, Smola JA, Ratsch G, Scholkopf B, Kohlmorgen J. Prediction time series with support vector machines. In: Scholkopf B, Smola AJ, editors. Advances in kernel methods. London, England: The MIT Press; 1999. p. 243–54.

[14] Mukherjee S, Osuna E, Girosi F. Non-linear prediction of chaotic time series using support vector machines. Proceedings of the IEEE NNSP'97, Amelia Island, FL, 1997.

[15] Joachimes T. Text categorization with support vector machines. Technical report, 1997. ftp: = =ftp-ai.informatik.uni-dortmund.-de = pub = Reports = report23.ps.z.

[16] Goldberg DE. Genetic algorithms in search, optimization and machine learning, vol. 77. Reading, MA: Addison-Wesley, 1989. p. 106–122.

[17] John CP. Sequential minimal optimization: a fast algorithm for training support vector machines. Technical report MSR-TR-98-14, April 21, 1998.

[18] Burge CJC. A tutorial on support vector machines for pattern recognition. Data Mining Knowledge Discovery 1998;2:121–67.

[19] Alex J, Smola, BS. A tutorial on support vector regression. NeuroCOLT2 technical report series NC2-TR-1998030, October, 1998.